Resistive transition process in granular superconducting MgB_2 films by analysis and simulation of the generated current noise

P. Mazzetti,[1,*] C. Gandini,[2] A. Masoero,[2] M. Rajteri,[3] and C. Portesi[3]
[1]*Politecnico di Torino, Dipartimento di Fisica, Corso Duca degli Abruzzi 24, 10129 Torino, Italy*
[2]*Università del Piemonte Orientale "Amedeo Avogadro," Dipartimento di Scienze e Tecnologie Avanzate–Centro Interdisciplinare Nano-SISTEMI, Via Bellini 25/G, 15100 Alessandria, Italy*
[3]*Istituto Nazionale di Ricerca Metrologica (INRIM), Strada delle Cacce 91, 10135 Torino, Italy*
(Received 3 October 2007; revised manuscript received 18 December 2007; published 26 February 2008)

An original model for the interpretation of the noise produced during the resistive transition of disordered granular MgB_2 superconductive films is presented and tested by comparison with extended experiments on these types of films. Both the amplitude and frequency behavior of the noise power spectrum, simulated on the basis of this model, are in very good agreement with the experimental results, practically without the introduction of adjustable parameters. The model is based on the onset of correlated transitions of large sets of grains, forming resistive layers through the film cross-section area during the transition process. The strong nonlinear behavior and correlation of the grains produces abrupt resistance variations, giving rise to the large noise, of the $1/f^3$ type, observed in experiments. These results show that, even in the case where the grain interface behaves as a strong link, as in MgB_2, if the grains are randomly oriented and are strongly anisotropic in regard to their critical current density, the transition models based on fluxoids depinning and motion, used for single crystals or grain oriented films, cannot be applied, at least when the transition takes place near the critical temperature at low bias currents. These models would justify a current noise power spectrum 2 or 3 orders of magnitude lower than the observed one in the low frequency range. Since the intrinsic superconductive properties of the material do not enter in its development, it is believed that this model may be generally applicable to disordered granular high-temperature superconductors, at least when the conditions of temperature and bias current specified above are met.

DOI: 10.1103/PhysRevB.77.064516 PACS number(s): 74.40.+k, 72.70.+m

I. INTRODUCTION

The study of the current or the magnetic noise produced in nonstationary conditions by slowly varying an external excitation applied to a complex system, particularly when it is in a critical state (e.g., during a superconductive or magnetic transition), is an important complement to the understanding of several transport and magnetic properties of such a system. Contrarily to the case of the noise taken in stationary conditions, which evidence reversible fluctuations of various properties characterizing the system, during the variation of an applied field or of the temperature, a complex system in general undergoes a sequence of internal configurational changes which correspond to the reaching of a local minimum of its free energy, giving rise to large fluctuations of different physical quantities associated to the system itself. This situation is related to the strong interaction existing between the constitutive elements of a complex system, which generates avalanche processes characterized by a noise power spectrum of the type $1/f^n$, with $n \geqslant 2$. This is, for instance, the case of the Barkhausen noise in ferromagnets, whose study did allow a good understanding of the dynamics of the Bloch walls in these materials, giving information not available with other types of measurements.[1–4]

For what concerns metallic type-II or single-crystal high-T_c superconductors (HTSs), most papers found in the literature are about noise measurements taken in stationary conditions, when the specimen is made resistive by the application of a constant magnetic field or a current density larger than the critical one at a given temperature. In this case a noise with a $1/f^n$ power spectrum with $1 \leqslant n \leqslant 2$ is generally found, and is interpreted according to different models, depending on the type and structure of the superconductor. The prevailing model is, in this case, depinning and motion of fluxoids generated by an external field or produced by the bias current near the transition temperature. The noise is produced by fluxoid density fluctuation and mutual fluxoid interaction, which can give rise to clustering and avalanche effects. Many theoretical studies and simulations of fluxoids motion with various arrangements of the pinning centers have been published[5–7] and used to interpret the magnetic and current noise both in conventional metallic superconductors and in single crystal or grain-oriented HTS thin films.[8–10] Flux noise measurements and evidence of avalanches involving a few thousands of fluxoids, produced by the application of a variable magnetic field, have been reported in metallic type-II superconductors by direct magnetic flux measurements.[11–15] These models have also been applied to interpret the noise generated in crystalline or high textured HTS thin films.[16–18]

A very different situation exists in the case of disordered granular HTS, both in the case where the grain interface behaves as a weak-link, as in YBCO,[19] or as a rather strong link, as in MgB_2.[20,21] For these materials the current noise generated in stationary conditions is generally interpreted on the basis of percolation-like models in the presence of temperature fluctuations[22–26] and is, almost invariably, of the $1/f$ type. A much larger noise is observed in these materials during the transition from the superconductive to the resistive state, or vice versa, induced by a slow variation of tempera-

ture, magnetic field, or current density. During the transition, a sequence of discrete rearrangements of the internal distribution of the current density occurs, giving rise to abrupt conductance changes and consequently to a large noise. In Ref. 27 a bulk YBCO specimen has been represented as a three-dimensional network of strongly nonlinear resistors, representing the weak-links as Josephson-like junctions, submitted to a variable magnetic field. Numerical solutions of the Kirchhoff's equations did show that, in this case, the transition is not a smooth process and evidenced the presence of several conductance steps of the network during field variation, in agreement with the current noise spectrum experimentally observed on the specimen, which was of the $1/f^2$ type. These steps correspond to the reaching of successive momentary equilibrium conditions of the current density distribution inside the specimen, following the variation of the weak-links critical current distribution induced by the variation of the applied magnetic field. It is interesting to notice, for a comparison with the results of the completely different approach described in this paper, that the number of steps coming out from the calculations were very nearly correspondent to the number of nodes of the network along the direction of the current flow. This fact, which was not taken into consideration in that occasion, assumes a particular meaning in relation to the present approach, since these steps seem to correspond just to the formation of the resistive layers described in Sec. III.

The present paper concerns the study of the noise produced during the transition from the superconductive to the resistive state in disordered nanogranular films of MgB_2, with the purpose of developing and testing a model apt to describe the main aspects of the transition process in similar types of HTS films. Even if, as in the case of MgB_2, the material is characterized by strong links, the anisotropy of the grain critical current density ($J_c^{ab}/J_c^c = 1.5-1.7$ for MgB_2, Refs. 28 and 29) prevents to consider the film as a uniform means with a suitable distribution of fluxoid pinning centers. Evidence that near the critical temperature the intergrain interface behaves as a weak-link even in the case of MgB_2 films is reported in Ref. 30.

As in YBCO specimens, also in the case of these films, during the transition, a large noise, indicative of the presence of avalanche processes, is observed. At low frequency the power spectrum of this noise, which is, in an extended frequency interval, of the $1/f^3$ type, is up to 3 orders of magnitude larger than the $1/f$ noise measured in stationary conditions. The experimental results, obtained under different physical conditions, are interpreted on the basis of a rather simple model, which is described in Secs. III and IV, and which gives the correct slope and amplitude of the power spectrum of the noise, practically without free parameters. All the parameters introduced in the theory are obtained either directly from the experimental data on the MgB_2 films or from known results reported in the literature. It is worth to notice that the good agreement between calculated and measured values of the amplitude of the noise power spectrum is a more stringent check for the theory than the one concerning its frequency behavior, since it is directly related to the magnitude of the avalanche processes produced during the transition. According to the model, this amplitude can be calculated from the data relative to the film dimensions, average grain size, and film electrical resistance in its normal state.

Alternative models, based on the noise generated by the motion of fluxoids in a matrix of pinning centers,[8–10] would predict a much lower noise amplitude, of the same order of magnitude of the noise taken in stationary conditions. Actually, even if fluxoids avalanche effects have been experimentally observed, as in Refs. 11 and 12, or expected on the basis of simulations, as in Ref. 9, the number of fluxoids involved in each avalanche is by far not enough to account for the noise intensity observed during the transition process. While the behavior of the noise power spectrum can be simulated in a limited frequency interval, its amplitude is in general expressed in arbitrary units.

The transition model proposed in this paper has been developed and tested under the assumption that the transition takes place near to the critical temperature, with low values of the bias current and in the absence of a magnetic field. A different situation, where fluxoids depinning and motion could become the dominant effect, at least at the beginning of the transition, might occur if the transition takes place at much lower temperatures, in the presence of strong magnetic fields or high current densities. In this case a two stage transition is expected, since the emf generated by fluxoid motion must, at a given point of the transition, become a potential drop in a normally resistive material. Owing to heating effects, the measurement of the transition noise with a constant bias current may become, in this case, a very difficult task.

II. EXPERIMENTAL

In order to make a good check of the model described in the next sections, we report here a set of experimental results relative to the measurement of electrical resistance and current noise power spectrum during the resistive transition of two MgB_2 superconductive specimens having different physical characteristics.

MgB_2 thin films have been prepared at the INRIM Laboratories by a growth process on silicon nitride substrates. Mg an B were simultaneously evaporated on a SiN substrate kept at 650 K. In order to get good structural and electrical properties of the films, Mg and B precursors were annealed *in situ* at 890 K for 600 s in argon atmosphere at a pressure of 1 mbar.

The films thickness was measured with a Tencor profilometer. Each MgB_2 film was patterned by standard lithography and etched in a solution of 1% HCl in water. The two specimens *S*1 and *S*2 had the same surface, a square of 1×1 mm^2 placed between two larger areas used for separated current an voltage contacts, but were characterized by a different thickness (30 and 100 nm, respectively) and by the same average grain size. Grain size was evaluated jointly with a STM and x-ray diffraction techniques. STM revealed clusters of grains of the order of 50–100 nm, while x rays assured that grain size was below 20 nm. By analogy with Ref. 30, where a more sophisticated analysis with a TEM techniques revealed an average grain size below 10 nm, we

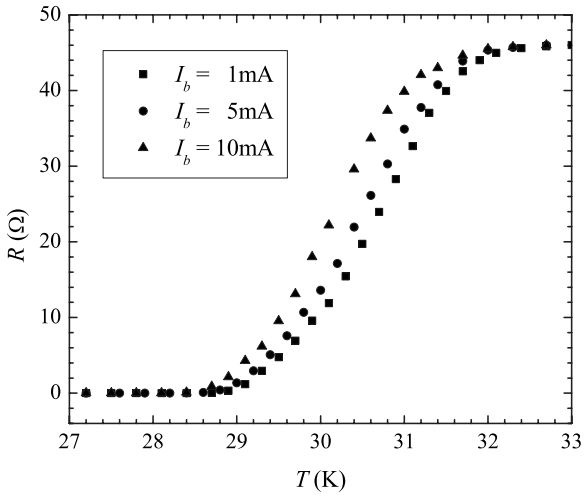

FIG. 1. Transition curves of specimen $S1$ for different values of the bias current I_b. These curves will be used to obtain the value of some of the parameters needed to evaluate the noise power spectra according to the proposed model, as described in Sec. V.

assumed, to make a comparison with the results of our model about the amplitude of the transition noise, an average grain size of 10 nm. Resistance and noise measurements were performed by means of a standard four contact technique. Each specimen was sealed within a copper container filled with helium and put in a cryostat with the possibility of slowly changing the temperature across its critical value. During noise measurements, in order to avoid spurious temperature fluctuations, a spontaneous temperature increase was obtained by switching off the cryocooler. Temperature was measured by means of a silicon diode sensor placed very close to the sample, and the electrical resistance R by means of a separated current source and a nanovoltmeter. Thermoelectric emf was canceled by the current reversal method. Temperature variation rate dT/dt near the superconductive-resistive transition was 0.033 K s^{-1}.

Figures 1 and 2 show the resistive transition for three different bias currents of film $S1$ and $S2$, respectively. The observed shift of the curves toward lower temperatures when the current density increases, were used to determine the

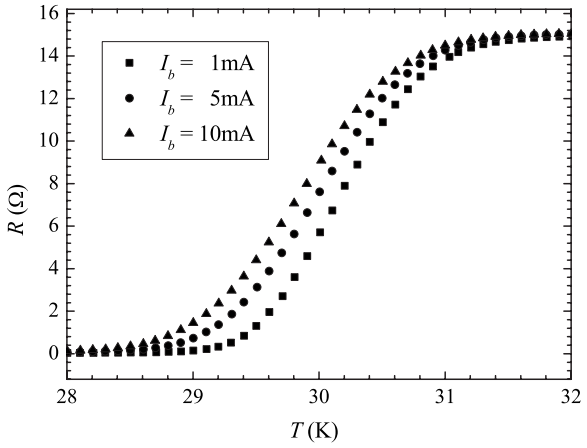

FIG. 2. Same as Fig. 1 for specimen $S2$.

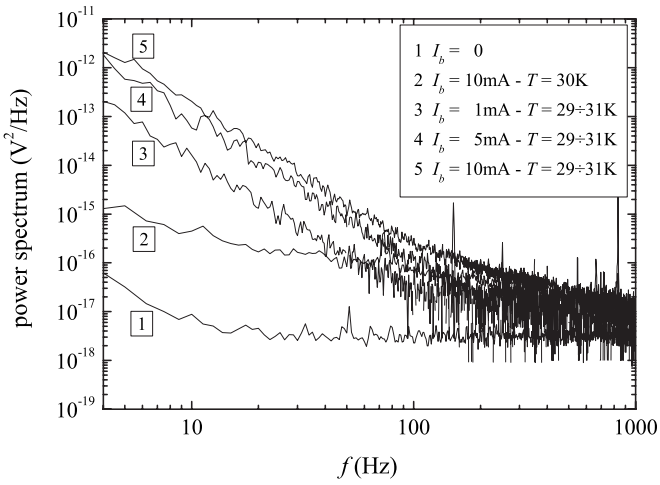

FIG. 3. Noise power spectra of the MgB_2 superconductive film $S1$, whose characteristics are given in the text. Curves 3, 4, 5 represent the noise spectra during the transition in the temperature interval between 29 and 31 K, while curve 2 represents the noise spectrum in stationary conditions at the temperature of 30 K. I_b is the bias current applied to the specimen. The background noise spectrum, represented by curve 1, has been subtracted to all the other spectra.

relation between critical temperature and critical current density appearing in the model described in the next section and used in the simulations reported in Sec. V.

An extra low noise step-up transformer (PAR Mod. AM-1) was used to detect the noise signal during the transition and to act as an high-pass filter to suppress the dc component of the spectrum. Its low frequency cutoff was about 4 Hz. In order to make a correction at low frequencies, the detected power spectra of the noise were divided by the square of the frequency transfer function $H(f)$ of the transformer. This function, which represents the ratio between the output and input sinusoidal signals of the transformer at any given frequency f, was measured according to the usual techniques, using the appropriate input and output impedances. A constant current generator was used to bias the specimen, and an HP signal analyzer (HP Mod. 3562A) to obtain the noise power spectrum.

In Figs. 3 and 4 the power spectra of the noise, corrected for the transformer transfer function, are reported. It can be noticed that in stationary conditions (constant temperature, in the middle of the resistive transition) the power spectrum is very nearly of the $1/f$ type, while, during the transition, a much larger noise, which is of the $1/f^3$ type in the low-frequency range, can be observed. Actually the whole spectrum can be interpreted as the superposition of a spectral component of the $1/f^3$ type, generated during the transition, superimposed to the $1/f$ spectral component observed in stationary conditions. It may also be observed that the amplitude of the power spectrum does not increase proportionally to the square value of the bias current, as would be expected if the resistance fluctuation is independent of the bias current. An interpretation of this behavior (which is in complete agreement with the proposed model) will be given in Sec. IV and proved by numerical simulation in Sec. V.

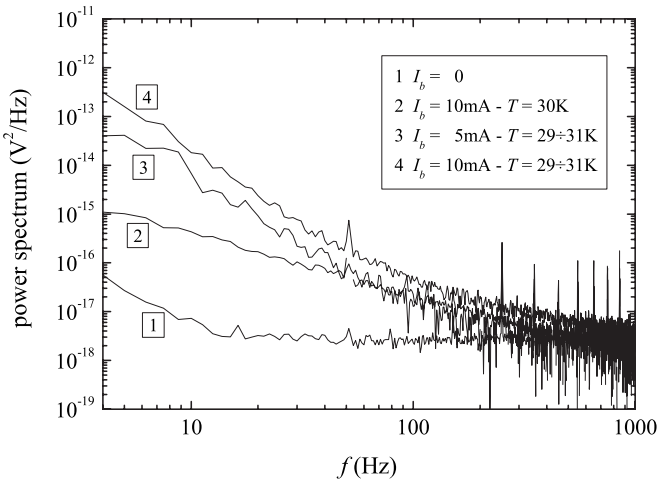

FIG. 4. Same as Fig. 3, but concerning the specimen *S*2. Also for this specimen the transition noise spectra are of the $1/f^3$ type at low frequency. Their amplitude is reduced of a factor of about 10, as expected from the theory reported in the following.

III. DESCRIPTION OF THE INTERPRETATIVE MODEL

In this section a model is proposed which, taking into account the granular structure and the physical characteristics of this type of superconductors, gives a consistent interpretation of the physical processes taking place during their resistive transition. In particular the model explains the origin of the large noise produced during the transition and gives a noise power spectrum which is quantitatively in good agreement with the experimental results for what concerns both its shape and amplitude. The type of approach is not very different from the one used in Ref. 31 to explain the resistance anisotropy of YBCO specimens submitted to a magnetic field.

The specimen will be considered as a three-dimensional array of MgB_2 grains $\{i\}$ randomly oriented, characterized by a critical current $I_c^i(T)$, which depends on their relative orientation with respect to the local direction of the current density and from small variations of their stoichiometry. Since grains are very small (about 10 nm in the present case) the current density can be considered uniform within the grain volume, and thus a critical current for each grain can be defined. Furthermore, without loss of generality for what concerns the model development, the grains can be considered as having all the same size and the same resistance R_g when in their normal state. The *I*-*V* characteristic of the grain transition is assumed to be similar to the one of a Josephson junction, and is schematically represented in the inset of Fig. 5. It is completely determined by $I_c^i(T)$ and R_g.[35] Depending on the temperature and bias current of the sample, the grain can be in one of these three states: superconductive, intermediate, and fully resistive. The last condition is realized when the grain resistance reaches its normal value R_g, while the intermediate state corresponds to the case where the current crossing the grain maintains its critical value $I_c^i(T)$, while the voltage drop varies between zero and $R_g I_c^i(T)$.

The model starts from the consideration that the sample, at an initial stage of its transition, can be considered as a sequence of equipotential regions made of grains all in the superconductive state, separated by resistive layers crossing the whole sample through its longitudinal direction, along which the bias current is flowing. The mechanism of formation of a resistive layer can be described as follows. During the temperature increase near T_c, the critical current of each grain lowers according to Eq. (1) and, at a given time, a layer of contiguous grains crossing the transversal section of the whole specimen occurs, where the sum of the critical currents of the grains is lower than the bias current applied to the specimen. At this point the layer becomes resistive. Since the potential drop across the layer should be the same for all the involved grains, because it separates two equipotential regions, it can be safely assumed that the layer is a sheet of single grains. The fact that these grains have different critical currents implies that, at the beginning of the transition, part of the grains are in a fully resistive state, while others are in an intermediate state. During the temperature increase, these last grains drift towards a fully resistive state, and the electrical resistance of the whole layer $\Delta R(T)$, after an abrupt step, increases slowly toward saturation (see Fig. 5).

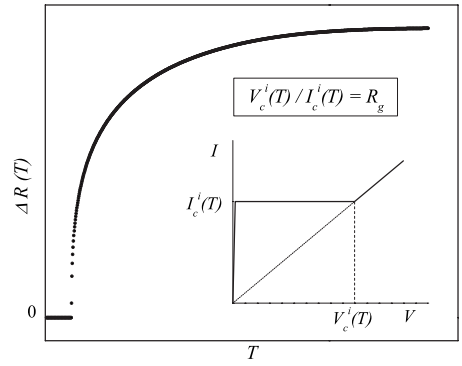

FIG. 5. Behavior of the resistance contribution of a single layer of resistive grains to the total resistance of the specimen vs temperature. The asymptotic approach to saturation is due to the presence of grains in the intermediate state, characterized by $V < V_c^i(T)$. The inset represents a draft of the *I*-*V* characteristic of an individual grain *i*. This characteristic, as stated in the text, is completely determined by the value of $I_c^i(T)$ and R_g.

The actual shape of the resistance pulse depends on the critical current distribution of the grains involved in the layer formation. Such a distribution, which is related to the random orientation of the grains,[28,29] is assumed to be represented by a Gaussian function, whose standard deviation is discussed in the following section.

There is another important point which must be taken into account. In order to explain the slope of the transition curves, which remains approximately constant even when the bias current becomes very small (see Figs. 1 and 2), it is necessary to assume that a distribution of the critical temperature T_c^i over the grain ensemble exists. The origin of this distribution is attributed to small variations of the grain stoichiometry related to the film deposition techniques.[32] In the model, also this distribution is assumed to be Gaussian and its standard deviation determined on the basis of the slope of the transition.

As described in detail in the next section, the transition from the superconductive to the normal state of the material

is represented as a sequence of processes corresponding to the creation of resistive layers. The resulting sequence of overlapping resistance steps gives rise to a progressive resistance increment for the whole specimen, with a superimposed voltage noise, whose power spectrum can be analytically evaluated under some simplifying assumptions.

IV. MODEL DEVELOPMENT

The first step for the evaluation of the power spectrum concerns the calculation of the shape of the voltage pulse produced when a resistive layer is generated. This requires of expressing the dependency of the grain critical current $I_c^i(T)$ and its distribution over $\{i\}$ on temperature. Within the interval of a few Kelvin near T_c, this dependency may be expressed, as a good approximation, by the linearized equation

$$I_c^i(T) = I_{c0}^i\left(\frac{T_c^i - T}{T_c^i}\right). \tag{1}$$

Owing to the electrical anisotropy of the grains, to their random orientation, and to fluctuations in their stoichiometry, both I_{c0}^i and T_c^i may be considered as distributed according to two Gaussian functions, whose standard deviations will be indicated by ΔI_{c0} and ΔT_c and their average values over the $\{i\}$ ensemble by I_{c0} and T_c. Consequently, according to Eq. (1), also $I_c^i(T)$, for each set of grains characterized by a given value of T_c, turns out to be distributed according to a Gaussian function of standard deviation $\Delta I_c(T)$ and mean value $I_c(T)$.

As discussed in detail in Sec. V, in the numerical implementation of the model, I_{c0} will be obtained from the shift of the transition curve along the temperature axis when the bias current I_b is changed, while the value of ΔI_{c0} is assumed on the basis of the critical current density anisotropy of crystalline MgB_2. Since ΔI_{c0}, similar to I_{c0}, are independent of temperature, the quantity $\Delta I_c(T)/I_c(T)$ remains a constant when the temperature T in Eq. (1) varies. This implies that the standard deviation $\Delta I_c(T)$ shrinks, together with $I_c(T)$, when the bias current I_b is reduced and the transition temperature increases. This gives rise to a steeper transition of the layer, as reported in Fig. 7 in Sec. V, a fact which has an influence on the noise power spectrum, giving a non quadratic dependence of its amplitude on the bias current (see Figs. 8–10 in Sec. V). The values of T_c and ΔT_c are obtained from the position and slope of the transition curve along the temperature axis for the lowest value of the bias current, when the effect of the grain critical current distribution becomes negligible. Since, in correspondence of the transition, T is very near to T_c^i and a small variation of T_c^i gives rise to a large relative variation of $I_c^i(T)$, it can be safely assumed that each layer is formed by grains having very nearly the same T_c and that subsequent layers formed during the transition, when the temperature increases, are constituted by grains having increasingly higher values of T_c.[36] In the following the critical temperature of the grains of a layer j will be indicated by $T_c^{(j)}$. The standard deviation ΔT_c of T_c is thus the parameter which determines the slope of the transition of the whole specimen, but not the one of a single layer.

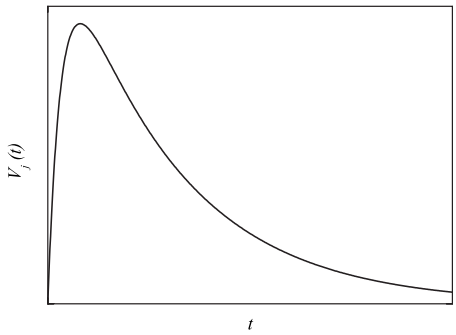

FIG. 6. Behavior of the voltage pulse generated by the formation of a single resistive layer. The trailing edge is related to the behavior of the curve represented in Fig. 5, once that the linear relation between time and temperature variation is taken into account. The exponential decay $\exp[-\beta t]$, needed to perform analytical calculation of the power spectrum, represents the effect of the low frequency cutoff of the transformer on the voltage pulses. After spectrum calculation, the limit $\beta \to 0$ is performed. This corresponds to the correction of the transformer effect on the experimental spectra, as discussed in the text.

The process of a layer formation, described in the preceding section, has been implemented with a MATLAB code, briefly described in Sec. V, and Fig. 5 represents an example of the outcome of the calculations for a given value of the bias current I_b and of the standard deviation of the grain critical current distribution. To avoid divergences in the analytical calculation of the power spectrum, each step, corresponding to the resistance increase produced by a layer formation, is assumed to decay to zero according to an exponential law of time constant τ_c. This decay produces a low frequency cutoff of the power spectrum below $f_c = 1/2\pi\tau_c$, which corresponds to the low frequency cutoff of the transformer (see Fig. 6).

After the evaluation of the analytical expression of the power spectrum, the limit $\beta = 1/\tau_c \to 0$, is performed. This operation corresponds to the correction of the experimental spectra by taking into account the frequency transfer function of the input transformer, as described in Sec. II, and shifts the divergence to $\omega = 0$. Thus the shape of the power spectrum depends only on the form of the trailing edge of the pulse. Assuming that the voltage pulses $V_j(t)$, produced by the formation of each resistive layer, are statistically independent processes, and thus distributed according to a Poisson law, the power spectrum simply becomes

$$\phi(\omega) = \nu\overline{|S_j(\omega)|^2}, \tag{2}$$

where ν represents the average number of pulses per unit time and $\overline{|S_j(\omega)|^2}$ the average square modulus of the Fourier transform of each pulse, given by

$$S_j(\omega) = \frac{1}{\sqrt{2\pi}}\int_{-\infty}^{+\infty} V_j(t)e^{-i\omega t}dt. \tag{3}$$

To the purpose of performing an analytical calculation, each pulse $V_j(t)$ is approximated by the following expression:

$$V_j(t) = B_j e^{-\beta t}\left[1 - \sum_{i=1}^{n} A_i e^{-\alpha_i t}\right] \tag{4}$$

with

$$\sum_{i=1}^{n} A_i = 1. \tag{5}$$

In Eq. (4) B_j represents the pulse amplitude in the limit $\beta \rightarrow 0$ and the quantity within square brackets represents a fitting of the trailing edge of the unitary pulse by means of n exponential functions of suitable amplitude A_i and time constant $1/\alpha_i$.

The value of B_j is not necessarily the same for the different layers. Actually the layers may be characterized by a different number of grains and give a different contribution to the film resistance change.

From Eqs. (2) and (4) a general expression of the power spectrum $\phi(\omega)$ has been worked out with a Macsyma program. When the limit $\beta \rightarrow 0$ is performed, this expression simply becomes

$$\phi(\omega) = \frac{1}{2\pi}\nu\overline{B_j^2} \times \left\{\left[\sum_{i=1}^{n} A_i \frac{\omega}{\omega^2 + \alpha_i^2} - \frac{1}{\omega}\right]^2 + \left[\sum_{i=1}^{n} A_i \frac{\alpha_i}{\omega^2 + \alpha_i^2}\right]^2\right\}. \tag{6}$$

The quantity $\nu\overline{B_j^2}$ can be expressed in terms of the film resistance R just before the superconductive transition, the average grain size s, the length of the sample L, the slope of the transition curve dR/dT within the temperature interval where the noise is detected, the rate of change of the temperature dT/dt and the value of the applied bias current I_b. Thus the mean value of the amplitude of the voltage pulses produced by the resistive transition of the layers is

$$\overline{\Delta V_j} = \overline{B_j} = I_b \frac{Rs}{L}, \tag{7}$$

while the average number of pulses per unit time ν is given by

$$\nu = \frac{L}{Rs}\frac{dR}{dt}. \tag{8}$$

Then

$$\nu(\overline{B_j})^2 = I_b^2 \frac{Rs}{L}\frac{dR}{dt} = I_b^2 \frac{Rs}{L}\frac{dR}{dT}\frac{dT}{dt} \approx \nu\overline{B_j^2}. \tag{9}$$

In Eq. (9), in order to make a comparison with the experimental results, the approximation $(\overline{\Delta V_j})^2 \approx \overline{(\Delta V_j)^2}$ has been performed. This approximation, which will be further discussed in Sec. VI, is justified by the fact that, in agreement with the assumptions reported above, the resistance increment produced by the formation of a resistive layer will be rather similar for each layer, except when the resistive transition of the whole specimen is almost complete and the creation of an individual layer loses its meaning. For these reasons, noise measurements were taken in a range of temperature variation excluding the upper part of the transition curve.

It is important to notice that the quantity $\nu\overline{B_j^2}$ represents the main amplitude factor for the noise power spectrum and that this quantity can be evaluated with a good approximation from the film dimensions, average grain size and electrical resistance in the normal state, without free parameters. The terms within curled brackets in Eq. (6) are only dependent on the shape of the trailing edge of the voltage pulse generated during the transition of a single layer. These terms give the frequency dependency of the power spectrum and have a smaller, even if not negligible, influence on its amplitude. Since the noise amplitude is strongly dependent on the type of model which is assumed for describing the transition process, the fair agreement between theory and experiments reported in the next section may be considered as a strong support to the model proposed in this paper.

V. DISCUSSION

In this section we shall make a direct comparison between experimental and theoretical results by applying the model described above to the specimens whose noise spectra are reported in Sec. II. In particular a detailed report is given for the case of specimen $S1$, observing that the spectra reported for $S2$ are similar in shape, while their amplitude is reduced of a factor of about 10. According to Eq. (9), being s, L and dT/dt equal quantities for both specimens, the amplitude factors $\nu\overline{B_j^2}$ of the corresponding spectra, at the same bias current, scale proportionally to RdR/dT. The average values of this quantity, taken over the transition curves of the two specimens, reported in Figs. 3 and 4, give a ratio of about 9, close to the experimental one. The actual values of these quantities can be evaluated, without free parameters, from the data given in Sec. II. From Eq. (9) it turns out that $\nu\overline{B_j^2} \approx \nu(\overline{B_j})^2 = 2.3 \times 10^{-4} \cdot I_b^2$ for specimen $S1$ and $2.5 \times 10^{-5} I_b^2$ for specimen $S2$.

As already stated, the terms within curled brackets in Eq. (6), in addition of giving the frequency behavior of the noise spectrum, have also an influence on its amplitude. Actually the spectrum appears as shifted towards higher frequencies along the x axis when the steepness of the pulse trailing edge increases. This effect is the reason why, even if $\nu\overline{B_j^2}$ is proportional to I_b^2, the power spectral density of the noise, at any given frequency, is not.

The behavior of the pulse trailing edge for different values of the bias current I_b is then calculated. The quantities characterizing the specimen $S1$, needed for this calculation, have been obtained from the transition curves reported in Fig. 1. The quantities I_{c0} and T_c, which represent the mean values of the quantities I_{c0}^i and T_c^i appearing in Eq. (1), have been obtained, respectively, from the shift of the transition curves along the temperature axis, when the bias current is changed, and from the average temperature of the transition curve at the lowest bias current: $I_b = 1$ mA. Taking into account that the temperature shift of the transition curves, when the bias current is changed from 1 to 10 mA, is approximately 0.54 K, and that T_c is 30.6 K, the coefficient I_{c0} in Eq. (1)

turns out to be $510/n_g$ mA, n_g being the average number of grains in a single layer.

Since in the numerical calculation of the trailing edge profile of the pulse the grain size s is not involved, in the simulation n_g has been chosen sufficiently large to obtain a correct use of the statistical distribution of the grain critical currents, but not necessarily so large as the real number is. In the present simulation n_g was taken to be 10^4, about two orders of magnitude lower than the real one. Checks were made to assure that an increase of n_g would not appreciably change the shape of the profile.

As stated in the preceding section, to evaluate the grain critical current distribution vs temperature through Eq. (1), I_{c0}^i is assumed to be expressed by a Gaussian function around its average value I_{c0}, with a standard deviation ΔI_{c0}. This last quantity, on the basis of the critical current density anisotropy for crystalline MgB_2, which is of the order of 1.5–1.7,[28,29] was assumed to be $0.4I_{c0}$. Further considerations on the value of this quantity, which can be considered the only best fit parameter used to fine trimmer the amplitude of the calculated noise spectra reported in Figs. 8–10, is given in the last section of the paper.

Finally, for the calculation of the trailing edge profile, the value of $T_c^{(j)}$, which characterizes an individual layer j, can be chosen equal to T_c, since different values of this quantity, within the Gaussian distribution of T_c^i, appearing in Eq. (1), simply shift the temperature at which the layer transition takes place, without altering the shape of the transition curve.

Having completely characterized all the quantities appearing in Eq. (1), the MATLAB calculation proceeds as follows. First the vector of the critical currents $I_c^j(T)$ is calculated for the n_g grains of the layer and for a given value of the temperature T by means of Eq. (1). The vector of the I_{c0}^j, in front of this equation is obtained as $I_{c0}^j = I_{c0}[1+\Delta I_{c0}\text{randn}(n_g,1)]$, where the MATLAB function randn$(n_g,1)$ gives a Gaussian vector of n_g elements of unitary standard deviation. The sum $S(T)=\Sigma_{j=1}^{n_g} I_c^j(T)$ is then calculated and compared with the bias current I_b. If $I_b \leqslant S(T)$, the layer is still superconductive, then T is increased until $I_b > S(T)$, and the layer becomes resistive.

At this point, using the I-V characteristic of each grain, which is completely determined by its critical current $I_c^j(T)$ (see Fig. 5), a value of the potential drop $\Delta V(T)$, equal for all the grains of the layer, is determined by means of an iterative routine in MATLAB, making use of the bisection method. The resistance of the layer at the temperature T is then given by $\Delta R(T)=\Delta V(T)/I_b$. With the increase of T an increasing number of grains of the layer are passing from an intermediate state, where $\Delta V < V_c$, to a fully resistive state, characterized by R_g, until ΔR reaches its saturation value.

Figure 7 shows the results for specimen $S1$, relative to the values of the bias current used in the experiments. The conversion from temperature to time was made by taking into account that the spontaneous rate of change of the specimen temperature dT/dt, near the transition, was +0.033 K s^{-1}, as reported in Sec. II. In order to evaluate the terms within curled brackets in Eq. (6), these curves have been fitted with three exponentials, whose amplitudes and time constants are reported in the figure caption.

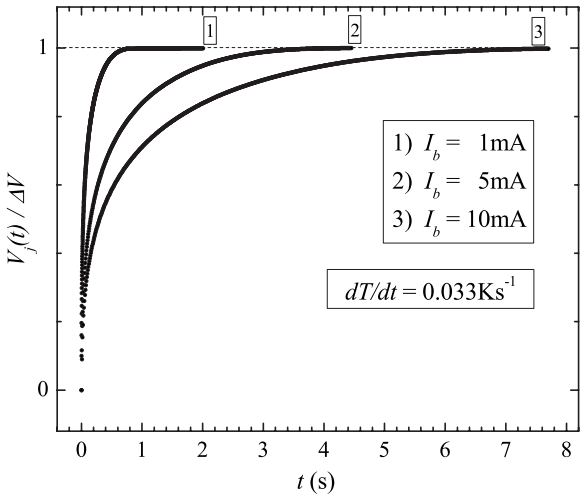

FIG. 7. Normalized trailing edge vs time of the unitary voltage pulse generated by the resistive transition of a single layer for different values of the bias current I_b and at a rate of change of the temperature of 0.033 K s^{-1}. For the analytical calculation of the power spectrum these curves have been fitted with the sum of three exponential functions, corresponding to the terms appearing within square brackets in Eq. (4). Curve 1: A_1=0.517, A_2=0.268, A_3 =0.215, α_1=5.83 s^{-1}, α_2=47.21 s^{-1}, α_3=535.10 s^{-1}. Curve 2: A_1 =0.519, A_2=0.265, A_3=0.216, α_1=1.17 s^{-1}, α_2=9.39 s^{-1}, α_3 =90.00 s^{-1}. Curve 3: A_1=0.517, A_2=0.267, A_3=0.216, α_1 =0.517 s^{-1}, α_2=4.68 s^{-1}, α_3=50.30 s^{-1}. The fitting curves are not shown in the figure since they practically overlap the original ones.

Equation (6) was then used to obtain the spectra reported in Figs. 8–10 for the three values of the bias current. To make a comparison with the experimental ones, the amplitude of these spectra has been corrected by a factor of 4π, in order to take into account that commercial spectrum analyz-

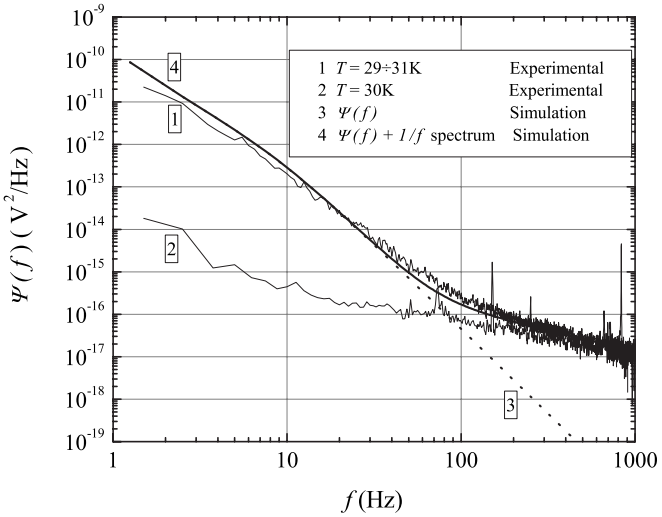

FIG. 8. Calculated power spectrum $\Psi(f)=4\pi\phi(\omega)$ of the noise generated during the transition of specimen $S1$ at I_b=10 mA (dotted curve 3). Full line (curve 4) represents the sum of $\Psi(f)$ with the smoothed out experimental $1/f$ spectrum measured in stationary conditions (curve 2). Curves 3 and 4 overlap below 35 Hz. The experimental power spectra given by curves 1 and 2 are the same as in Fig. 3.

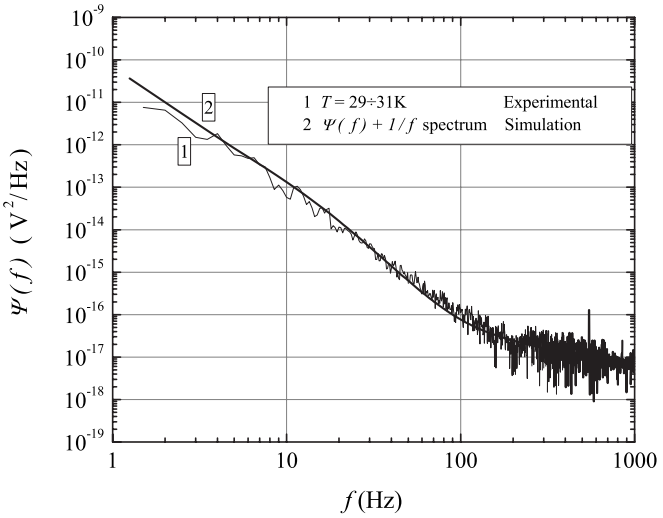

FIG. 9. Same as Fig. 8, but at I_b=5 mA.

ers produce a power spectrum $\Psi(f)$ which refers only to positive values of the frequency and is normalized in such a way that its integral over f, and not over ω, gives the power associated with the noise in any frequency range. Then $\Psi(f)=4\pi\phi(\omega)$.

In addition to the noise spectra, Eq. (1) can also be used to reproduce the transition curves given in Figs. 1 and 2. As already discussed in Sec. IV, the transition of the whole specimen is characterized by the fact that different layers, whose grains have increasingly higher values of $T_c^{(j)}$, make subsequent resistive transitions, when the temperature increases, until the whole specimen becomes fully resistive. This situation is still described by Eq. (1), by assuming that T_c^i is characterized by a Gaussian distribution of values with a standard deviation ΔT_c and mean value T_c. This standard deviation gives the mean slope of the transition curve, while the shift of the curve toward higher temperatures, when I_b is decreased, is determined by I_{c0}, whose value in Eq. (1) was already chosen on the basis of this shift of the experimental curves.

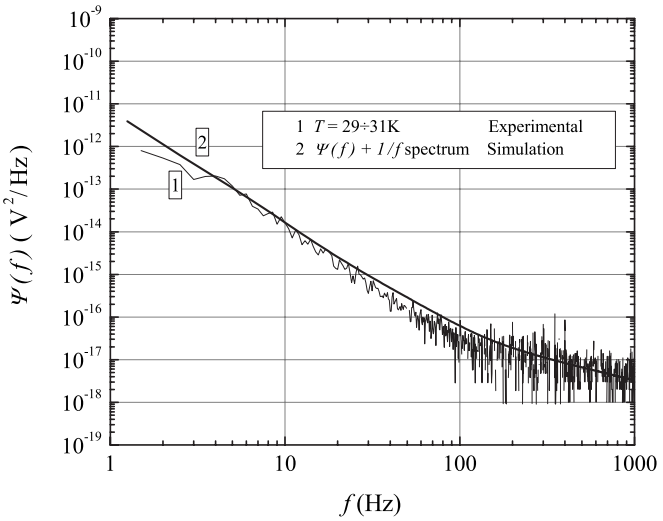

FIG. 10. Same as Fig. 8, but at I_b=1 mA.

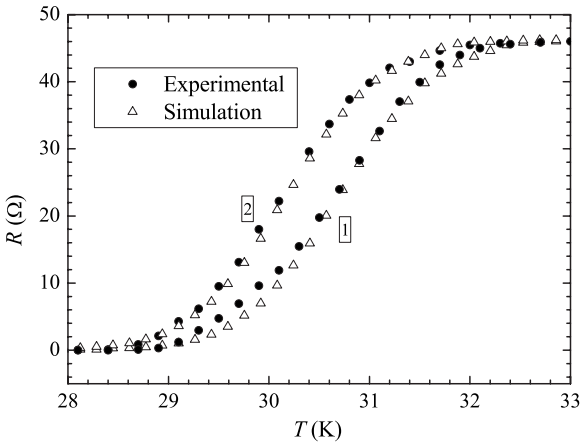

FIG. 11. Simulation of the specimen transition curves obtained by summing up the resistance increments due to subsequent transitions of the layers during the temperature increase. Calculations are based on Eq. (1) with the same values of the parameters used in the noise power spectra evaluation, and are described in detail in the text. Curves 1 and 2 correspond, respectively, to I_b=1 and 10 mA. Experimental curves are the same as reported in Fig. 1.

Calculation were made with a MATLAB program similar to the one described above, by making use of a matrix of critical currents, whose columns represent the vectors of the critical currents of the different layers on which the specimen is subdivided.

The curves reported in Fig. 11 have been obtained by assuming $\Delta T_c=0.026T_c$. The very good fit of the calculated curves to the experimental ones for what concerns their shift towards higher temperatures when I_b is lowered and their average slope, are not surprising, since they derive from the choice of I_{c0}, ΔI_{c0}, T_c and ΔT_c in Eq. (1), based on the experimental data. The S-like shape of the curves is mostly due to the Gaussian distribution of T_c^i. The profile of the layer transitions (see Fig. 5) gives also a contribution, but a smaller one.

Thus, while in this case the good agreement between the experimental and simulated curves may not be considered as a proof of the validity of the proposed model, it shows that this model is consistent also with these aspects of the experimental results, and that the values of the quantities used in Eq. (1) for the evaluation of the noise spectra are the correct ones also for this calculation. As already stressed in the preceding sections, it is the noise which gives the transition dynamics and can unambiguously prove, by means of its amplitude and frequency behavior, if a model may or may not reasonably explain the physics of the process.

VI. CONCLUSIONS

In this section we shall briefly summarize and comment the effect on the reported results of the assumptions which have been introduced in order to make the model tractable, such to allow of expressing the noise power spectrum in an analytical form. Two main assumptions were made to this purpose: (a) that the elementary events, corresponding to the formation of a resistive layer, could be considered as statis-

tical independent processes described by a Poisson distribution and (b) that the mean square value of the voltage pulses could be approximated by the square of their average value. Assumption (a) can be acceptable, except near the end of the transition, where, on the other side, the noise tends to vanish. Actually, when contiguous layers are not separated by superconductive regions, correlation effects may be created by the current density continuity relation. For this reason the noise power spectrum was taken not too near to saturation. Assumption (b) might give rise to a reduction of the amplitude of the spectra, but it certainly would not change the order of magnitude of this quantity. For instance, by assuming a Gaussian distribution of n_g over the different layers with a standard deviation $\Delta n_g = 0.5 n_g$, the noise spectral amplitude would be increased of only 25% with respect to the reported value, barely visible at the scale of the reported spectra. Also the dependency of ν on time during the transition can be disregarded in the frequency range of the reported spectra, since it would alter their shape below the frequency of its modulation, i.e., in the present case, below about 0.1 Hz. The last point that we will briefly discuss concerns the assumption of a Gaussian distribution for the grain critical currents at given temperature $T^{(j)}$, when the layer transition takes place. It may be observed that the grain random orientation would not produce a Gaussian distribution of critical currents and that a more accurate calculation should have been performed. The reason why this has not been done is because there is another quantity which has an indirect but large influence on the grain critical current at a given temperature, and it is the grain critical temperature T_c^i, whose standard deviation ΔT_c is related to the slope of the transition curves. Owing to the large impact that this quantity has on the grain critical current at a given temperature, as the results reported in Figs. 1 and 2 show, it has been assumed that each layer j is generated by grains having all the same value $T_c^{(j)}$, and that only during the temperature increase, layers characterized by increasingly higher values of $T_c^{(j)}$ may occur. However, if it is taken into account that small variations of $T_c^{(j)}$ are possible also for the grains belonging to the same layer, then the tails of a Gaussian function may be justified.

As a conclusion of this analysis, it can be stated that, for what concerns the power spectrum of the noise, both its amplitude and its frequency behavior are little affected by the simplifying assumptions listed above. The good agreement with the experimental results remains even if the quantity ΔI_{c0}, characterizing the distribution of the critical currents in a layer and the grain size s are reasonably changed. Therefore, even if the description of the transition dynamics of the film may appear oversimplified in this semiclassical approach, since quantum effects deriving from the proximity of the grains are disregarded, it seems that the main aspects of the process, deriving from the strong correlation existing between grain transitions during the layer formation, are correctly taken into account by the proposed model. For specimen $S1$, avalanches involving up to 10^6 grains are expected and give the correct order of magnitude for the amplitude of the noise power spectrum.

To complement this study, it would be useful to perform transition noise measurements on single crystals or grain oriented HTS films both in the presence and in the absence of a magnetic field. In this case the contribution of fluxoid creation, depinning and motion could become an important fraction of the transition process, at least in its initial stage, while the normal state of the material would be reached only near the end of the transition. Noise analysis could be perhaps the best, if not the unique, means of understanding what type of process takes place, since in the case of fluxoid motion, a much lower noise is expected, of the same order of magnitude of the stationary one. For the development of bolometric sensors based on HTS thin films, this type of knowledge would be very important in order to obtain an high signal to noise ratio.[33,34]

ACKNOWLEDGMENTS

The authors wish to thank Eugenio Monticone of INRIM for providing the MgB_2 films used in the reported experiments and for many useful discussions concerning this paper.

*piero.mazzetti@polito.it

[1] L. V. Meisel and P. J. Cote, Phys. Rev. B **46**, 10 822 (1992).
[2] S. Zapperi, P. Cizeau, G. Durin, and H. E. Stanley, Phys. Rev. B **58**, 6353 (1998).
[3] B. Tadic and U. Nowak, Phys. Rev. E **61**, 4610 (2000).
[4] S. L. A. de Queiroz and M. Bahiana, Phys. Rev. E **64**, 066127 (2001).
[5] C. Reichhardt, C. J. Olson, J. Groth, S. Field, and F. Nori, Phys. Rev. B **53**, R8898 (1996).
[6] C. J. Olson, G. T. Zimanyi, A. B. Kolton, and N. Gronbech-Jensen, Phys. Rev. Lett. **85**, 5416 (2000).
[7] Q. Lu, C. J. Olson Reichhardt, and C. Reichhardt, Phys. Rev. B **75**, 054502 (2007).
[8] R. Kato and Y. Enomoto, Physica C **426**, 110 (2005).
[9] C. J. Olson, C. Reichhardt, J. Groth, S. B. Field, and F. Nori, Physica C **290**, 89 (1997).
[10] J. Das, T. J. Bullard, and V. C. Täuber, Physica A **318**, 48 (2003).
[11] C. Heiden and G. I. Rochlin, Phys. Rev. Lett. **21**, 691 (1968).
[12] S. Field, J. Witt, F. Nori, and X. Ling, Phys. Rev. Lett. **74**, 1206 (1995).
[13] A. C. Marley, M. J. Higgins, and S. Bhattacharya, Phys. Rev. Lett. **74**, 3029 (1995).
[14] S. H. Chun, W. Song, G. H. Koh, H. C. Kim, and Z. G. Khim, Physica C **282-287**, 2335 (1997).
[15] G. Stan, S. B. Field, and J. M. Martinis, Phys. Rev. Lett. **92**, 097003 (2004).
[16] K. Frikach, A. Taufik, S. Senoussi, and A. Tirbiyin, Physica C **282-287**, 1977 (1997).
[17] Y. Togawa, R. Abiru, K. Iwaya, H. Kitano, and A. Maeda, Phys. Rev. Lett. **85**, 3716 (2000).
[18] A. Maeda, T. Tsuboi, R. Abiru, Y. Togawa, H. Kitano, K. Iwaya, and T. Hanaguri, Phys. Rev. B **65**, 054506 (2002).

[19] M. Tinkham and C. J. Lobb, *Solid State Physics* (Academic Press, New York, 1989), Vol. 42, p. 91.
[20] D. C. Larbalestrier, L. D. Cooley, M. O. Rikel, A. A. Polyanskii, J. Jiang, S. Patnaik, X. Y. Cai, D. M. Feldmann, A. Gurevich, A. A. Squitieri, M. T. Naus, C. B. Eom, E. E. Hellstrom, R. J. Cava, K. A. Regan, N. Rogado, M. A. Hayward, T. He, J. S. Slusky, P. Khalifah, K. Inumaru, and M. Haas, Nature (London) **410**, 186 (2001).
[21] Y Bugoslavsky, G. K. Perkins, X. Ql, L. F. Cohen, and A. D. Caplin, Nature (London) **410**, 563 (2001).
[22] J. H. Lee, S. C. Lee, and Z. G. Khim, Phys. Rev. B **40**, 6806 (1989).
[23] M. Celasco, A. Masoero, P. Mazzetti, and A. Stepanescu, Phys. Rev. B **44**, 5366 (1991).
[24] L. B. Kiss and P. Svedlindh, Phys. Rev. Lett. **71**, 2817 (1993).
[25] L. Cattaneo, M. Celasco, A. Masoero, P. Mazzetti, I. Puica, and A. Stepanescu, Physica C **267**, 127 (1996).
[26] G. Leroy, J. Gest, L. K. J. Vandamme, and J.-C. Carru, Physica C **425**, 27 (2005).
[27] P. Mazzetti, A. Stepanescu, P. Tura, A. Masoero, and I. Puica, Phys. Rev. B **65**, 132512 (2002).
[28] S. Sen, A. Singh, D. K. Aswal, S. K. Gupta, J. V. Yakhmi, V. C. Sahni, E.-M. Choi, H.-J. Kim, K. H. P. Kim, H.-S. Lee, W. N. Kang, and S.-I. Lee, Phys. Rev. B **65**, 214521 (2002).
[29] O. F. de Lima and C. A. Cardoso, Physica C **386**, 575 (2003).
[30] S. Chromik, S. Gazi, V. Strbik, M. Spankova, I. Vavra, S. Benacka, J. C. van der Beek, and P. Gierlowski, J. Appl. Phys. **96**, 4668 (2004).
[31] D. Daghero, P. Mazzetti, A. Stepanescu, P. Tura, and A. Masoero, Phys. Rev. B **66**, 184514 (2002).
[32] W. D. Markiewicz and J. Toth, Cryogenics **46**, 468 (2006).
[33] A. J. Kreisler and A. Gaugue, Supercond. Sci. Technol. **13**, 1235 (2000).
[34] F. Rahman, Contemp. Phys. **47**, 181 (2006).
[35] More realistically, the constant current part of this characteristic may actually be chosen with the current I slowly increasing with V, without appreciably changing the results of the reported results, as proved by numerical calculations.
[36] This assumption also solves the problem of applying Eq. (1) to the grains where $T_c^i < T$. Actually, most of these grains belong to layers which are already resistive and are in a fully resistive state. Isolated ones behave as holes in a superconductive matrix.